SUMOylation inhibitor TAK-981 (subasumstat) synergizes with 5-azacytidine in preclinical models of acute myeloid leukemia

Ludovic Gabellier,[1,2*] Marion De Toledo,[1*] Mehuli Chakraborty,[1] Dana Akl,[1] Rawan Hallal,[1] Mays Aqrouq,[1] Giovanni Buonocore,[1] Clara Recasens-Zorzo,[1] Guillaume Cartron,[1,2] Abigaïl Delort,[3] Marc Piechaczyk,[1] Denis Tempé[1] and Guillaume Bossis[1]

[1]IGMM, University of Montpellier, CNRS; [2]Service d'Hématologie Clinique, CHU de Montpellier and [3]MGX, University of Montpellier, CNRS, INSERM, Montpellier, France

*LG and MDT contributed equally as first authors.

Correspondence: M. De Toledo
marion.detoledo@igmm.cnrs.fr

D. Tempé
denis.tempe@igmm.cnrs.fr

G. Bossis
guillaume.bossis@igmm.cnrs.fr

Received: January 6, 2023.
Accepted: August 16, 2023.
Early view: August 24, 2023.

https://doi.org/10.3324/haematol.2023.282704

Abstract

Acute myeloid leukemias (AML) are severe hematomalignancies with dismal prognosis. The post-translational modification SUMOylation plays key roles in leukemogenesis and AML response to therapies. Here, we show that TAK-981 (subasumstat), a first-in-class SUMOylation inhibitor, is endowed with potent anti-leukemic activity in various preclinical models of AML. TAK-981 targets AML cell lines and patient blast cells *in vitro* and *in vivo* in xenografted mice with minimal toxicity on normal hematopoietic cells. Moreover, it synergizes with 5-azacytidine (AZA), a DNA-hypomethylating agent now used in combination with the BCL-2 inhibitor venetoclax to treat AML patients unfit for standard chemotherapies. Interestingly, TAK-981+AZA combination shows higher anti-leukemic activity than AZA+venetoclax combination both *in vitro* and *in vivo*, at least in the models tested. Mechanistically, TAK-981 potentiates the transcriptional reprogramming induced by AZA, promoting apoptosis, alteration of the cell cycle and differentiation of the leukemic cells. In addition, TAK-981+AZA treatment induces many genes linked to inflammation and immune response pathways. In particular, this leads to the secretion of type-I interferon by AML cells. Finally, TAK-981+AZA induces the expression of natural killer-activating ligands (MICA/B) and adhesion proteins (ICAM-1) at the surface of AML cells. Consistently, TAK-981+AZA-treated AML cells activate natural killer cells and increase their cytotoxic activity. Targeting SUMOylation with TAK-981 may thus be a promising strategy to both sensitize AML cells to AZA and reduce their immune-escape capacities.

Introduction

Acute myeloid leukemias (AML) are severe hematologic malignancies resulting from the acquisition of oncogenic mutations by hematopoietic stem or progenitor cells. AML cells, which are blocked at intermediate stages of differentiation, proliferate and infiltrate the bone marrow, thereby disrupting normal hematopoiesis.[1] Fit patients are usually treated with intensive chemotherapy based on the combination of an anthracycline (daunorubicin [DNR] or idarubicin) and the nucleoside analogue, cytarabine (ARA-C). Relapses are, however, frequent and overall survival (OS) remains very poor. In the past few years, various new molecules improving AML prognosis have been approved. In most cases, they target mutated oncogenes such as *IDH1/2* or *FLT3*, which restricts their use to patients carrying these mutations.[2] Unfit patients who cannot receive chemotherapy because of age or comorbidities are generally treated with hypomethylating agents, in particular 5-azacytidine (AZA).[3] In cells, this cytidine analog is metabolized into 5-aza-dCTP and incorporated into DNA during replication, where it can form covalent adducts with DNA-methyl transferases (DNMT). This triggers ubiquitin-proteasome-dependent depletion of DNMT[4] and results in a progressive

loss of DNA methylation at CpG dinucleotide motifs. The prevalent model to explain the therapeutic effect of AZA is that reduced methylation of CpG leads to the reactivation of silenced tumor suppressor genes as well as genes involved in differentiation, which are generally hypermethylated at *cis*-regulatory regions in cancer cells.[5] The clinical benefit of AZA treatment is, however, limited with a 4- to 5-month increased OS compared to other AML therapies.[6] Its combination with the BCL2 inhibitor venetoclax (VEN) significantly improves patient response and OS.[7,8] This combo is now used as first-line therapy for patients unfit for standard chemotherapies. Nevertheless, a proportion of AML patients respond poorly to this regimen or acquire resistance.[9,10]

SUMO proteins are peptide post-translational modifiers with structural homology to ubiquitin. Whilst human genome encodes for five SUMO genes (*SUMO-1* to *-5*), the main conjugated isoforms are SUMO-1, -2 and -3, the latter two being almost identical.[11] SUMOylation involves a SUMO-activating E1 enzyme (UBA2/SAE1), a SUMO-conjugating E2 enzyme (UBC9) and several E3 factors. SUMOylation is highly dynamic thanks to various isopeptidases, which can release SUMO from conjugated targets. SUMO are conjugated to lysines of thousands of proteins (>6,000 identified in cancer cells,[12] around 1,000 in healthy mouse tissues[13]) to modify their function and fate.[14] As such, SUMOylation has been implicated in the regulation of most cellular functions.[11] One of its best-characterized roles concerns the regulation of gene expression.[15,16] We have previously shown that SUMOylation limits the anti-leukemic activity of both chemotherapies (DNR and Ara-C)[17] and differentiation therapies[18] in AML. This suggested that targeting the SUMO pathway could improve AML responses to therapies.

A recent breakthrough in the field of SUMOylation is the discovery of TAK-981 (subasumstat), a first-in-class SUMO E1 inhibitor with very high potency and specificity.[19] TAK-981 has potent anti-tumoral activity in syngenic mouse models grafted with murine lymphoma or pancreatic tumor cells through the induction of a strong type-1 interferon (IFN-I)-dependent anti-tumor immune response.[20,21] Indeed, TAK-981 activates dendritic cells, cytotoxic $CD8^+$ T cells, memory B cells, natural killer (NK) cells and macrophages.[20-24] Moreover, TAK-981 increases antigen presentation by cancer cells, further enhancing anti-tumor immune response.[22] In addition to these effects on the immune micro-environment, TAK-981 can directly induce cancer cells death.[21,25-27] However, the relative contribution of the direct and indirect anti-tumoral activities of TAK-981 remains to be clarified.

Here, we have addressed the therapeutic potential of TAK-981 in AML. We found that TAK-981 has potent anti-leukemic activity, in particular when combined with AZA. TAK-981 exacerbates the transcriptional reprogramming induced by AZA. In addition to genes involved in differentiation and apoptosis, TAK-981+AZA induces inflammation- and immune response-related transcriptional programs. In particular, AML cells exposed to TAK-981+AZA show increased secretion of IFN-I. Finally, they express, at their membrane, NK adhesion molecules (ICAM-1) and ligands of NK activating receptors (MICA/B), leading to an enhanced NK cell-mediated cytotoxicity towards AML cells. Altogether, our data suggest that combining the inhibition of SUMOylation by TAK-981 and DNA methylation by AZA could be a promising strategy for AML treatment.

Methods

Bioluminescent cell line generation, patient cell cultures, flow cytometry and RNA-sequencing (RNA-seq) analysis are described in the *Online Supplemental Appendix*.

Pharmacological inhibitors and reagents

TAK-981 was obtained from Takeda Development Center Americas, Inc. and 5-azacytidine (AZA) was from StemCell and resuspended in RPMI prior to each experiment. DNR and aracytine (aracytosine-β-D-arabinofuranoside-ARA-C) were from Sigma-Aldrich, VEN from MedChemExpress. All antibodies used are described in *Online Supplementary Table S1*.

Cell lines and culture conditions

Human AML cell lines (U937, THP-1, HL-60, MOLM14, MV4.11) were obtained by the American Type Culture Collection and regularly tested for *Mycoplasma* contamination. They were cultured as previously described[28] at 37°C in the presence of 5% CO_2 in RPMI 1640 medium supplemented with 10% heat-decomplemented fetal bovine serum, penicillin and streptomycin. Cells were seeded at $0.3x10^6$/mL 1 day before being drug-treated.

Patient and healthy donor samples

Bone marrow aspirates and blood samples were collected after obtaining written informed consent from patients or donors under the frame of the Declaration of Helsinki and after approval by the Institutional Review Board (Ethical Committee "Sud Méditerranée 1," ref 2013-A00260-45, HemoDiag collection). Healthy donor leukocytes were collected from blood donors of the Montpellier Etablissement Français du Sang. Fresh leukocytes were purified by density based centrifugation using Histopaque 1077 (Sigma Aldrich). NK cells were purified using EasySep Human NK Cell Isolation kit (StemCell Technologies).

Acute myeloid leukemia mouse xenograft model

All experiments on animals were approved by the Ethics Committee of the Languedoc-Roussillon (2018043021198029 #14905 v3). For cell line-derived xenograft (CLDX) and patient-derived xenograft (PDX) experiments, female NOD/LtSz-SCID/IL-2Rγchain null (NSG) mice (Charles River) (6-10

weeks old) were treated using respectively 20 mg/kg and 30 mg/kg busulfan intravenous injections (SIGMA B2635, France) 48 hours before cell engraftment. $1x10^6$ cells (cell lines) or $1.5x10^6$ cells (patient's cells) were injected in the tail vein.

Assessment of natural killer cell cytotoxicity towards acute myeloid leukemia cells

Target cells (THP-1-LucZsGreen) were co-cultured at a 1:1 ratio in 96-well plates with primary NK cells purified from fresh peripheral blood mononucelar cells (PBMC) of healthy donors. Real-time fluorescence was assessed for 15 hours using the IncuCyte S3 Live Cell imaging system (Sartorius) in the non-adherent cell-by-cell mode, using a 20X objective, four images/well and one image/hour. Analyses were performed by measuring the relative integrated green fluorescence intensity using IncuCyte 2021C software.

Statistical analyses

Statistical analyses of the differences between data sets were performed using one-way ANOVA for normal distribution data and Kruskal-Wallis or Friedman tests for non-Gaussian distribution data (GraphPad Prism, GraphPad v9.4.0). Overall mouse survivals were estimated for each treatment group using the Kaplan-Meier method and compared with the log-rank test. *P* values of less than 0.05 were considered significant (*P< 0.05; **P< 0.01 and ***P< 0.001; NS: not significant).

Results

TAK-981 synergizes with 5-azacytidine to induce acute myeloid leukemia cell death *in vitro*

In order to characterize the effect of the SUMOylation inhibitor TAK-981 on AML cells, we first monitored its impact on SUMOylation in three model AML cell lines, HL-60, U937 and THP-1. After 24 hours, TAK-981 induced a strong decrease in global SUMOylation by SUMO-1 and SUMO-2/3 at 10 nM and an almost complete loss at 100 nM (Figure 1A; *Online Supplementary Figure S1A*). Although the extent of deSUMOylation was similar between the three cell lines, U937 and THP-1 cells were highly sensitive to TAK-981, whilst HL-60 were unaffected after 24 hours of treatment (Figure 1B). Importantly, TAK-981 did not significantly affect the viability of normal mononuclear cells derived from either bone marrow (BMDMC) or peripheral blood (PBMC) under the same conditions (Figure 1C). Then, in order to determine whether SUMOylation inhibition could synergize with the drugs most commonly used for AML treatment, we combined TAK-981 with either DNR, ARA-C or AZA to treat HL-60, the least sensitive cell line to TAK-981, for 24 hours (Figure 1D; *Online Supplementary Figure S1C*). TAK-981 synergized with all three drugs, the strongest synergy being with AZA (Figures 1D).

As several rounds of replication are necessary to obtain maximal AZA-induced hypomethylation, we performed viability assays after 72 hours of treatment. Under these conditions, all cell lines showed sensitivity to TAK-981 alone, HL-60 and U937 being however less sensitive than THP-1 cells (*Online Supplementary Figure S1B*). A synergistic cytotoxicity was seen between TAK-981 and AZA for these three cell lines (Figures 1E; *Online Supplementary Figure S1D*). TAK-981 and AZA combination was also more efficient than the single treatments on MOLM14 and MV4.11 cell lines (*Online Supplementary Figure S1E*). For all cell lines, AZA+TAK-981 combination was more efficient than AZA+VEN combination at decreasing AML cell line viability *in vitro* (note the differences in VEN and TAK-981 doses used; *Online Supplementary Figure S1E*). We then treated primary AML cells from 17 different patients. Both AZA and TAK-981 treatment led to a significant reduction in the number of leukemic cells, but the most important effect was obtained with the combination of the two drugs, with however some variability between patient samples (Figure 1F; *Online Supplementary Table S2*). This variability might be related to the cytogenetic characteristics of the patients, as those with abnormal karyotypes were more sensitive to TAK-981+AZA than those with a normal karyotype (*Online Supplementary Figure S2A*). In addition, patients from the more differentiated M4/M5 subgroups of French American British (FAB) classification were more sensitive to TAK-981 than those from the more immature M1/M2 subgroups (*Online Supplementary Figure S2B*). Finally, treatments had no significant effects on bone marrow-derived mononuclear cells (BMMC) from healthy donors cultured under the same conditions, although TAK-981, when used alone, tend to slightly increase their numbers (Figure 1G). Altogether, these data suggest that inhibition of SUMOylation with TAK-981 affects the viability of AML cells and synergizes *in vitro* with the hypomethylating agent AZA.

TAK-981 +5-azacytidine combination has anti-leukemic activity in preclinical acute myeloid leukemia models

In order to further delineate the therapeutical potential of the TAK-981+AZA combination, we performed *in vivo* experiments using NOD-SCID-gammaIL2R^{null} (NSG) mice. First, to ensure the efficiency of TAK-981 *in vivo*, we used a microbead-based assay[29,30] to monitor its ability to inhibit SUMOylation activity. TAK-981 treatment led to a 70% decrease in SUMOylation activity in the bone marrow of NSG mice after 5 hours and a progressive recovery to basal levels after 24 hours (*Online Supplementary Figure S3A*). Second, NSG mice were grafted intravenously with bioluminescent THP-1 (*Online Supplementary Figure S3B*) or U937 cells (O*nline Supplementary Figure S4A*). TAK-981 and AZA monotherapies limited tumor progression (Figure 2A; *Online Supplementary Figures 3C* and *S4B, C*) and significantly extended mice survival (Figure 2B; *Online Supplementary Figure S4D*) for both THP-1 and U937. TAK-981+AZA com-

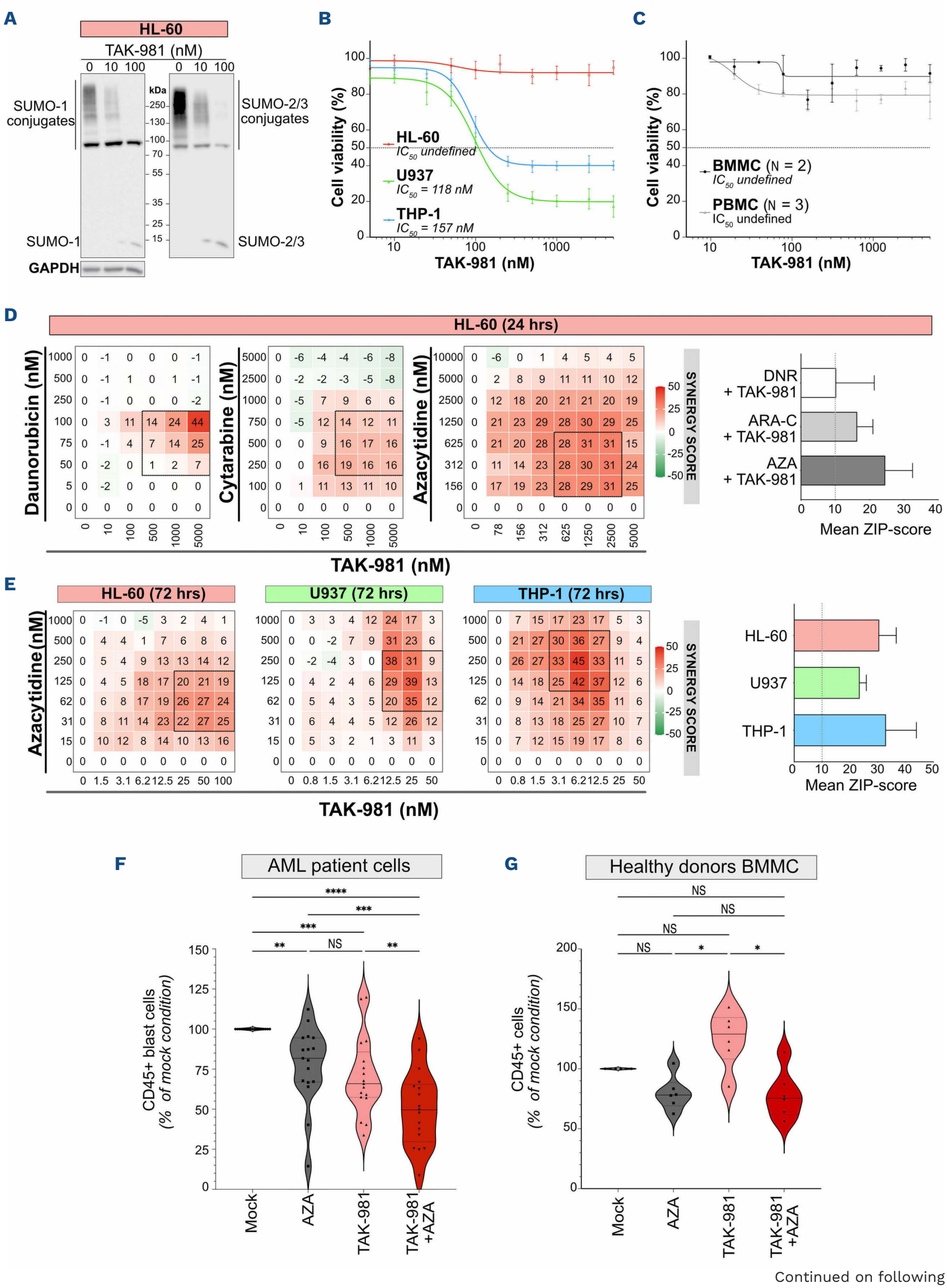

Continued on following page.

Figure 1. TAK981 synergizes with 5-azacytidine to induce acute myeloid leukemia cell death *in vitro*. (A) HL-60 cells were treated with increasing doses of TAK-981 for 24 hours and immunoblotted for SUMO-1, SUMO-2/3 and GAPDH. SUMO conjugates appear as smears. (B) TAK-981 half-maximal inhibitory concentrations (IC_{50}) were determined using HL-60, U937 and THP-1 cells treated with varying drug concentrations. Cell viability was determined using MTS assays after 24 hours of treatment. Concentration response curves were generated by comparing the viability of TAK-981-treated cells with mock-treated controls. Data are shown as mean +/- standard error of the mean (SEM) of replicate samples (N=5). Absolute IC_{50} are indicated in the figure. (C) Bone marrow-derived mononuclear cells (BMMC) (N=2) and peripheral blood mononulcear cells (PBMC) (N=3) collected from healthy donors were treated with varying TAK-981 concentrations for 24 hours. Cell viability was determined by flow cytometry after 24 hours of treatment. Concentration response curves were generated by comparing the viability of TAK-981-treated cells with mock-treated controls. Data are shown as mean +/- SEM of replicate samples. (D) HL-60 cells were treated for 24 hours with TAK-981 and either daunorubicin (DNR), cytarabine (ARA-C) or 5-azacytidine (AZA) and viability was assessed by MTS assay (median of 3 independent experiments for each drug). Left panels: heat maps showing the synergy ZIP-score between the 2 drugs, and the "most synergistic areas" (black squares) estimated using the SynergyFinder software v2.0. Right panel: mean of synergy ZIP-scores in most synergistic areas for HL-60 cells. Data are shown as mean +/- standard deviation (SD) of replicate samples (N=3 for each drug). Dotted line at 10% represents the threshold for significant synergy. (E) HL-60, U937 and THP-1 cells were treated with TAK-981 and AZA every day for 3 consecutive days. Viability was analyzed at day 4 and compared to that in mock-treated conditions (median of 3 independent experiments for each cell line). Left panels: heat maps for the corresponding synergy ZIP-score between the TAK-981 and AZA, and the "most synergistic areas" (black squares) estimated using the SynergyFinder software v2.0. Right panel: mean of synergy ZIP-scores in most synergistic areas for the 3 cell lines. Data are shown as mean +/- SD of replicate samples (N=3 for each cell line). Dotted line at 10% represents the threshold for significant synergy. (F, G) Patient (N=17) (F) or healthy donor (N=6) (G) BMMC were treated for 3 consecutive days (day 1, 2, 3) with TAK-981 (10 nM) and/or AZA (100 nM) and kept in culture. After 8 days, cells were collected and the number of $CD45^+$ cells was analyzed by flow cytometry in each condition and compared to the mock-treated condition. For each group, plain lines represent the median value, and dotted lines are the quartiles. Groups were compared using RM one-way ANOVA test.

bination had a much higher anti-leukemic effect than the monotherapies (Figure 2A, B; *Online Supplementary Figure 4B, D*). Finally, it was also more efficient than VEN+AZA combination at both limiting THP-1 cells proliferation *in vivo* and extending mice survival (Figure 2C, D; *Online Supplementary Figure S3D*).

We then turned to PDX (*Online Supplementary Table S2*). Once engrafted patient cells became detectable in blood, mice were treated with one cycle of TAK-981 and/or AZA and the number of leukemic cells was analyzed in spleen and bone marrow. For the first patient tested (PDX #1), TAK-981 decreased tumor burden on its own in the spleen. TAK-981+AZA treatment was more efficient than TAK-981 alone at decreasing tumor burden in both spleen and bone marrow (Figure 2E). Similar results were obtained with two other PDX (PDX #2 and PDX #3) (Figure 2F; *Online Supplementary Figure S4E*). AZA was highly efficient on its own on one of them (PDX #3), thus limiting the benefit of its combination with TAK-981 in this case (*Online Supplementary Figure S4E*). Altogether, these data show in preclinical models that targeting SUMOylation with TAK-981 can exert an anti-leukemic effect *in vivo*, which is increased when combined with AZA.

TAK-981 amplifies 5-azacytidine-induced transcriptional reprogramming and favors apoptosis

In order to study the molecular mechanisms underlying the synergy between TAK-981 and AZA in AML, we performed RNA-seq experiments in U937 cells treated for 72 hours. TAK-981 showed limited effects on gene expression with 112 genes upregulated and three genes downregulated more than 2-fold (Figure 3A). AZA induced a much broader transcriptional reprogramming with 1,684 genes up- and 225 genes downregulated (Figure 3B). The highest impact on transcription occurred with the TAK-981+AZA combo, with 2947 genes upregulated and 850 genes downregulated more than 2-fold (Figure 3C; *Online Supplementary Table S3*). Most genes up- or downregulated upon AZA (orange and purple dots, respectively) had higher fold changes upon TAK-981+AZA combination (Figure 3D). This suggests that inhibition of SUMOylation with TAK-981 amplifies AZA-induced modulation of gene expression. Accordingly, gene set enrichment analysis (GSEA) revealed that most gene signatures enriched in AZA-treated cells have higher normalized enrichment scores (NES) upon TAK-981+AZA treatment (Figure 3E). The most enriched pathways in the TAK-981+AZA *versus* mock- (Figure 3E), AZA- (*Online Supplementary Figure S5A*) and TAK-981- (*Online Supplementary Figure S5B*) treated cells, are linked to cell death as well as inflammation and immune system (see below). In order to avoid measuring transcriptional effects indirectly linked to the induction of cell death, we performed the RNA-seq analysis in U937 treated with doses of AZA and TAK-981 (10 nM each) suboptimal to induce apoptosis (Figure 4A). However, in line with the activation of transcriptional programs related to cell death, combinations of AZA and TAK-981 at higher doses led to a massive apoptosis both in U937 and THP-1 cells (Figure 4A). For both cell lines, TAK-981+AZA was more efficient than VEN+AZA at inducing apoptosis (Figure 4A). Finally, the most downregulated gene signatures in TAK-981+AZA treated cells are related to cell cycle progression, in particular MYC and E2F target genes (Figure 3E; *Online Supplementary Figure S3A, B*). We confirmed that c-MYC itself is downregulated upon TAK-981+AZA treatment in U937 cells (*Online Supplementary Figure S5C*). In the THP-1 and HL-60 cell line, we did not observe a significant modulation of c-MYC but TAK-981+AZA induced a strong up-regulation of *CDKN1a*, which encodes the $p21^{(WAF1/CIP1)}$ cell

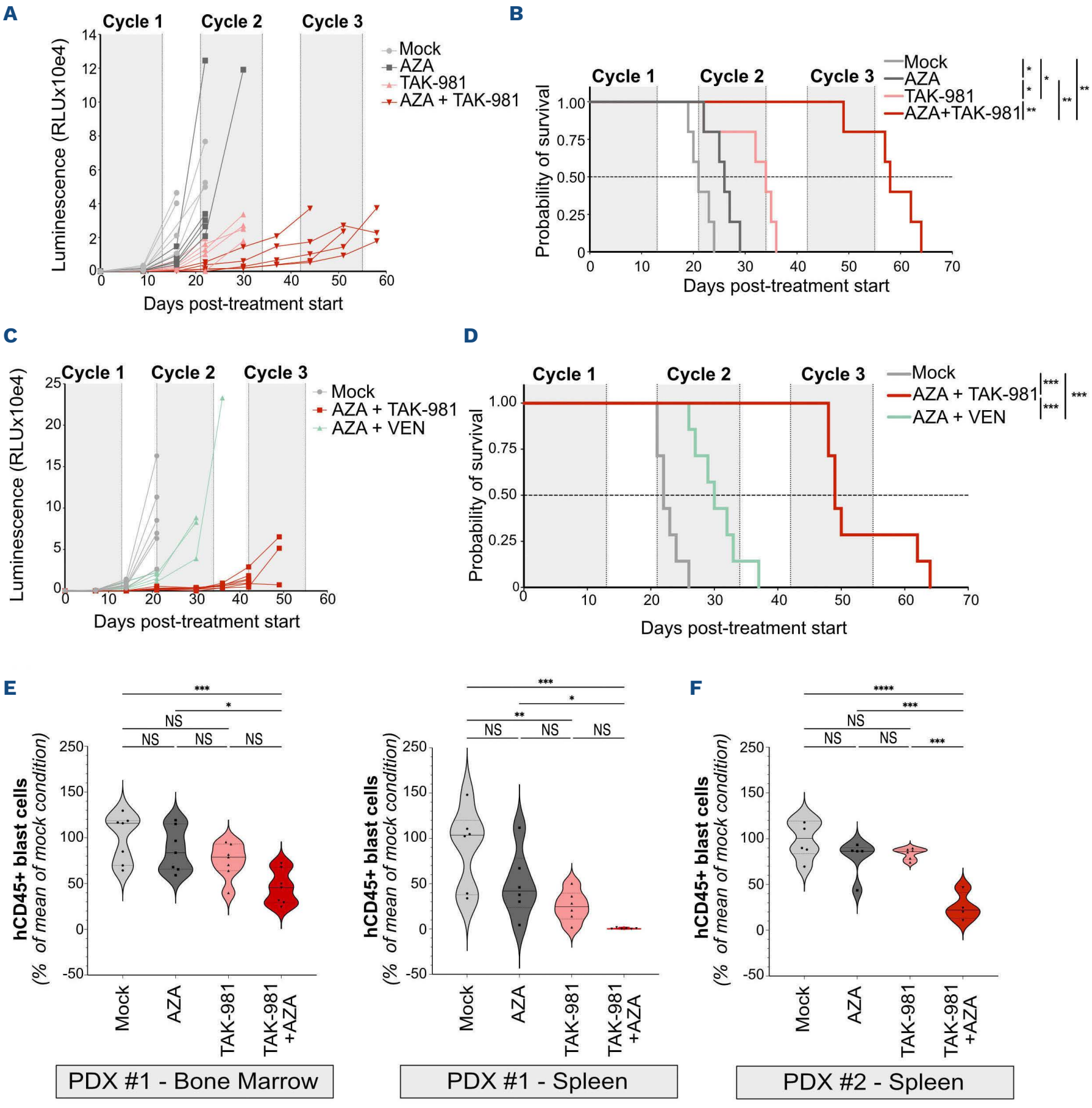

Figure 2. TAK-981 and 5-azacytidine combination has a higher anti-leukemic activity than monotherapies *in vivo*. (A, B) NSG mice were injected with THP-1 cells and treated with TAK-981 (15 mg/kg, intravenously [IV]), 5-azacytidine (AZA) (2 mg/kg, intraperitoneally [IP]) or the combination according to the schedule presented in *Online Supplementary Figure S2B* (N=5/group). (A) Quantification, as relative luminescence units, of tumor burden evolution monitored by luminescence intensity in mice injected with bioluminescent THP-1 cells. (B) Overall survival after treatment start of mice injected with bioluminescent THP-1 cells was estimated in each group and compared using Kaplan-Meier method and log-rank test. (C, D) NSG mice were injected with THP-1 cells and treated with TAK-981 (15 mg/kg, IV) and AZA (2 mg/kg, IP) or venetoclax (VEN) (50 mg/kg, oral gavage [OG]) according to the schedule presented in *Online Supplementary Figure S2D* (N=7/group). (C) Quantification (as relative luminescence units) of tumor burden evolution monitored by luminescence intensity in mice injected with bioluminescent THP-1 cells. (D) Overall survival after treatment start of mice injected with bioluminescent THP-1 cells was estimated in each group of treatment and compared using Kaplan-Meier method and log-rank test. (E, F) NSG mice were injected with primary cells from 2 different AML patients. After engraftment, mice were treated with AZA and/or TAK-981 and euthanized at day 9. The total number of human CD45$^+$ cells (hCD45) was estimated by flow cytometry in bone marrow (PDX #1, N=7) and spleen (PDX #1, N=6; PDX #2, N=4-6), and compared to the mean number of cells collected in the mock-treated group of mice. For each group, plain lines represent the median value, and dotted lines are the quartiles. Groups were compared using ordinary one-way ANOVA test.

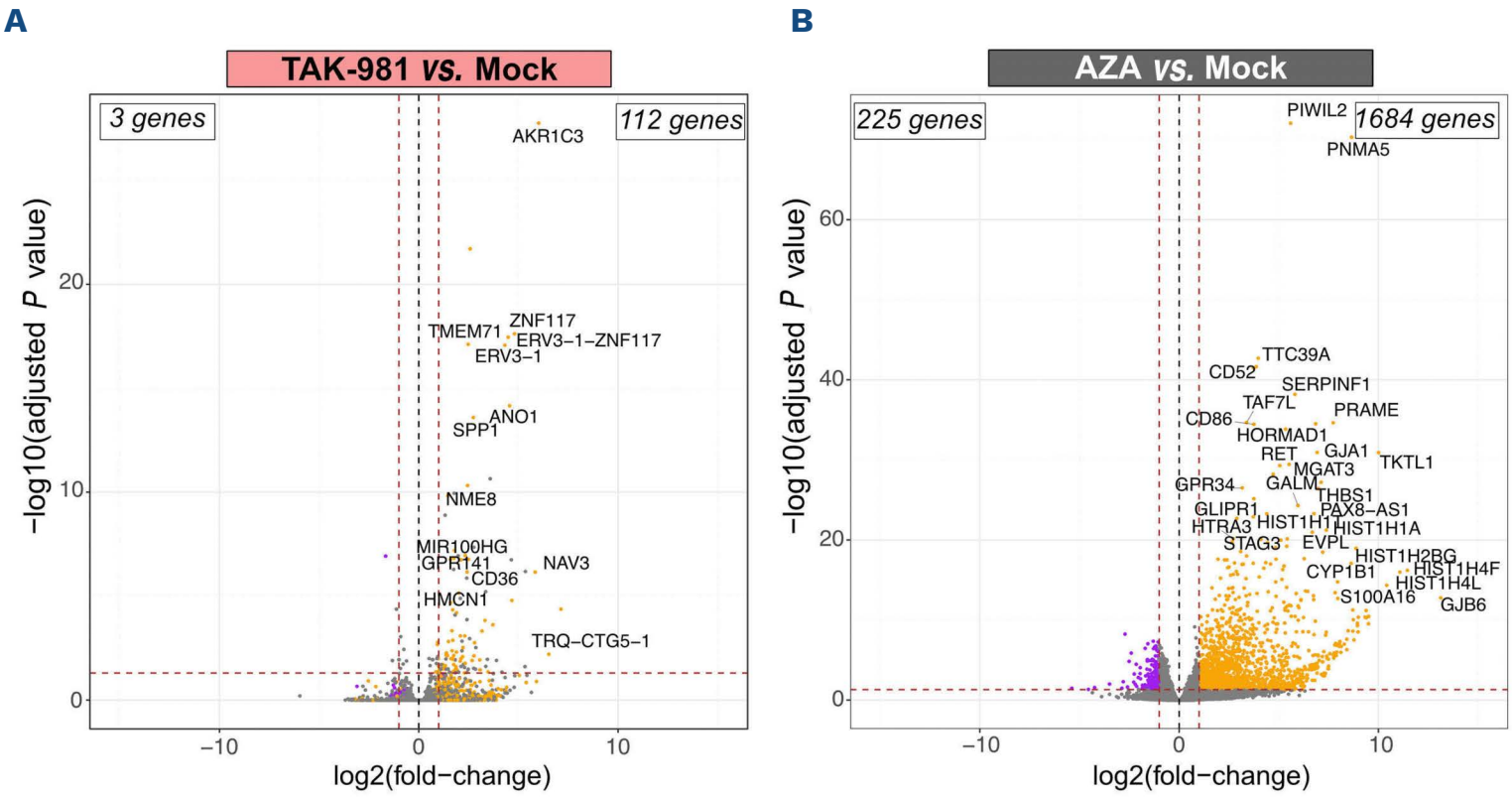

Continued on following page.

Figure 3. TAK-981 enhances 5-azacytidine-induced transcriptional reprogramming in U937 acute myeloid leukemia cell line. (A, B, C) Volcano plots showing differentially expressed genes (DEG) in U937 cell line treated each day for 3 days with 5-azacytidine (AZA) (10 nM) (A), TAK-981 (10 nM) (B) or the combination TAK-981+AZA (10 nM each) (C), analyzed at day 4 by RNA-sequencing and compared to mock-treated cells (N=3). Red dotted lines indicate the 2-fold change cutoff (absolute $\log_2$ fold change [abs $\log_2$FC]=1) and a *P* value of 0.05 ($\log_{10}$=1.3). The total numbers of up- and downregulated DEG are indicated. Orange and violet dots indicate genes whose expression is respectively up- or downregulated more than 2-fold by AZA-alone treatment. (D) Scatter plot displaying the DESeq2 fold change of DEG in TAK-981+AZA treated U937 cells as a function of their fold change in AZA-treated cells. The red line represents the linear regression of the fold changes for the comparison of AZA+TAK-981 *versus* AZA replicates. As a control, the grey line represents the linear regression from the comparison of AZA *versus* AZA replicates. *P* value was calculated using student *t* test between the two linear regressions. (E) Gene set enrichment analysis was performed using Hallmark datasets on the RNA-sequencing data obtained from U937 cells. All pathways significantly enriched in the AZA+TAK-981 compared to mock-treated cells are shown (absolute normalized enrichment score [abs NES]>1, *P*<0.05 and false discovery rate [FDR]<0.05). NES and FDR are also indicated for the AZA and TAK-981 *versus* mock-treated cells.

cycle inhibitor and is known to be repressed by c-MYC,[31] suggesting a downregulation of the MYC pathway in these cell lines as well (*Online Supplementary Figure 5D*). TAK-981, in particular when combined with AZA, altered cell cycle progression with decreased percentage of cells in G1 (Figure 4B). Altogether, this suggests that the amplification of AZA-induced transcriptional reprogramming by TAK-981 leads to decreased proliferation and increased apoptosis of the leukemic cells, providing an explanation for the synergy between the two drugs.

TAK-981+5-azacytidine favors acute myeloid leukemia cell differentiation

Restoration of differentiation participates to the anti-leukemic action of various drugs, including hypomethylating agents.[32] Gene signatures related to myeloid differentiation were enriched in TAK-981+AZA compared to mock, AZA and TAK-981 treatments (Figure 5A; *Online Supplementary Table S4*). We confirmed by quantitative reverse transcription polymerase chain reaction (qRT-PCR) that TAK-981+AZA combo leads to a stronger increase in the expression of the myeloid marker CD14 compared to the single treatments in U937 cells (Figure 5B). TAK-981+AZA also induced CD14 expression at the surface of U937 xenografted in mice (Figure 5C). Similarly, CD14 expression was found induced in THP-1 cells, with again a maximal effect obtained for the TAK-981+AZA combination (Figure 5D). As a comparison, VEN+AZA combination also induced CD14 expression in THP-1 cells at however lower levels (*Online Supplementary Figure S6*). Finally, the prodifferentiation effect of TAK-981+AZA treatment was confirmed on patient cells *in vivo*, both in the blood (Figure 5E) and bone marrow (Figure 5F) of PDX mice (PDX #1), with increased expression of CD14 and CD15 at the surface of the leukemic cells. Altogether, our data suggest that the anti-leukemic action of the combination of TAK-981 and AZA is associated to the reactivation of leukemic cells differentiation.

TAK-981+5-azacytidine induces the secretion of type-1 interferon by acute myeloid leukemia cells

As mentioned above, inhibition of SUMOylation increases AZA-induced expression of genes linked to inflammatory response and immunity (Figure 3E). In particular, this concerns IFN-I response pathway (Figure 6A), with genes such as interferon regulatory factors (IRF) being maximally upregulated upon TAK-981+AZA in both U937 (Figure 6B) and THP-1 cells (Figures 6C, D). Accordingly, TAK-981+AZA induced the production of IFN-α by THP1-cells (Figure 6E). We then analyzed IFN-α production *in vivo* by intracellular labeling of IFN-I on AML patient cells recovered from the bone marrow of PDX mice (PDX #1). Only TAK-981+AZA induced an increase in IFN-α production by the AML cells (Figure 6F).

Thus, in addition to a direct effect on AML cells differentiation, proliferation and viability, TAK-981+AZA combination enhances the secretion of IFN-I by AML cells, which may stimulate innate and/or adaptive anti-tumor immune response.

TAK-981 induces the expression of natural killer cell ligands on acute myeloid leukemia cells and activates natural killer cell cytotoxicity

NK cells play critical roles in cancer immune surveillance, including in AML.[33] Within the gene signatures linked to immune response enriched in TAK-981+AZA *versus* mock-, AZA- or TAK-981-treated U937 cells, we identified several related to the activation of NK cells (Figure 7A; *Online Supplementary Table S4*). Among the genes of this signature, we focused on the adhesion molecule ICAM-1, which is required for target cells to bind to NK through its interaction with LFA-1,[34] as well as on the MICA/B ligands of the NK-activating receptor NKG2D present on NK cells.[35] TAK-981 increased the expression of ICAM-1 and MICA/B at the surface of THP-1 cells, which was further increased by addition of AZA (Figures 7B, C). *In vivo*, ICAM-1 expression at the surface of xenografted patient cells was also increased by both TAK-981 and TAK-981+AZA treatments (Figure 7D) whereas, only TAK-981+AZA led to an increased MICA/B expression (Figure 7E). In order to assess whether these treatments could enhance the activation of NK cells, we co-cultured PBMC purified from the blood of six different healthy donors as a source of NK cells together with THP-1 cells, previously treated with TAK-981, AZA or the drugs combination. The expression of the activation marker CD69 was increased at the surface of NK cells when they were co-cultured with TAK-981- or TAK-981+AZA-treated THP-1

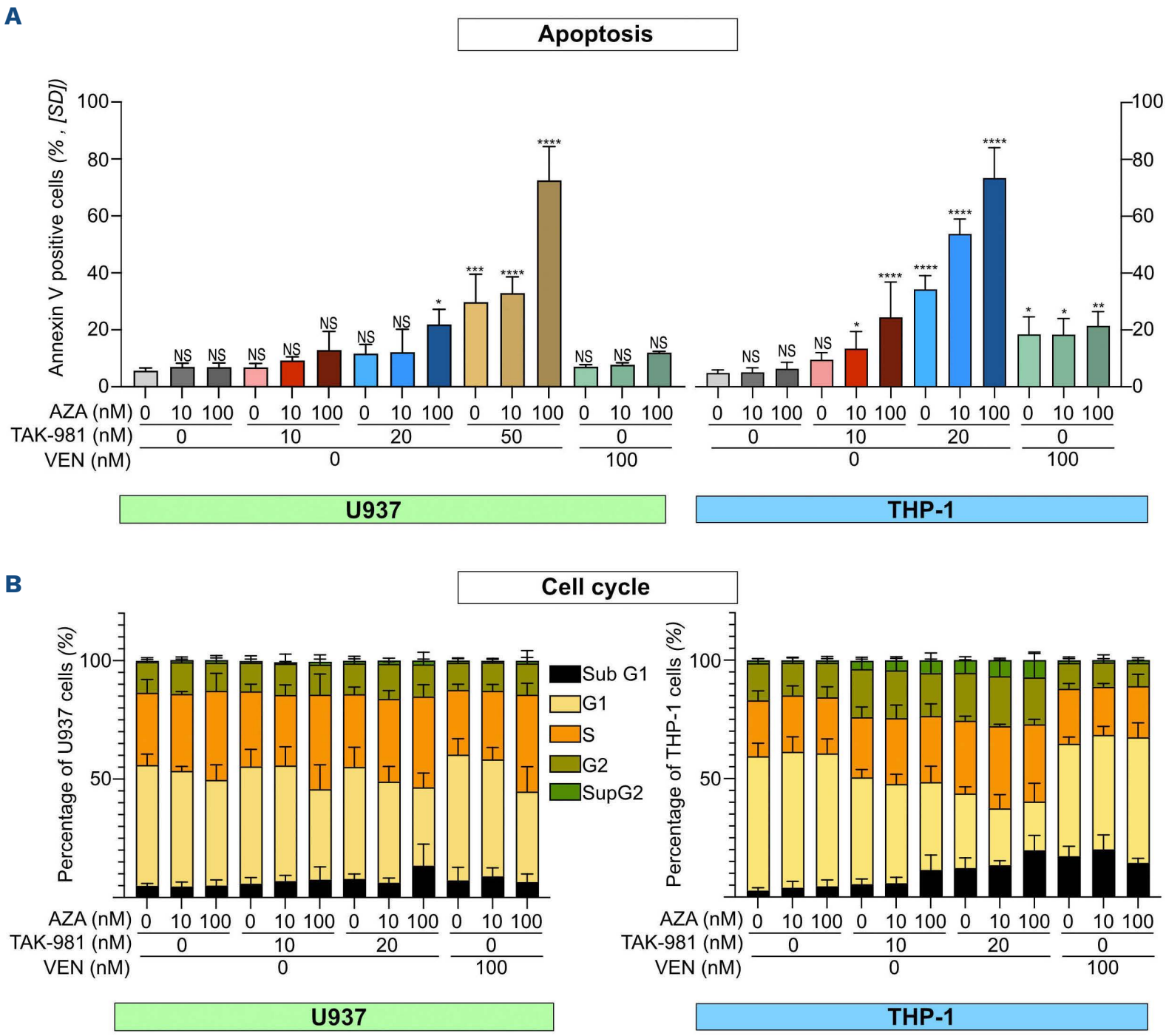

Figure 4. TAK-981+5-azacytidine induces apoptosis and cell cycle defects in acute myeloid leukemia cells. (A) U937 or THP1 cells were treated every day for 3 consecutive days with TAK-981, 5-azacytidine (AZA) or venetoclax (VEN) at the indicated doses and stained on day 4 with Annexin-V/7AAD to quantify apoptotic and dead cells (N=3, mean +/- standard deviation [SD], conditions were compared to mock-treated condition using ordinary one-way ANOVA). (B) Cells treated as in (A) were stained with propidium iodide to analyze cell cycle distribution (N=3, mean +/- SD).

compared to mock- or AZA-treated cells (Figure 7F). Finally, we monitored the cytotoxicity of purified NK cells isolated from five healthy donors towards THP-1 cells using live cell imaging. NK cell cytotoxicity was higher on THP-1 cells that had been previously treated with TAK-981+/-AZA compared to mock- or AZA-treated cells (Figures 7G, H). Altogether, our data suggest that TAK-981+AZA favors the recognition and lysis of AML cells by NK cells, which could contribute to the anti-leukemic activity of this treatment.

Discussion

Here, we report that the SUMOylation inhibitor TAK-981 has anti-leukemic activity in various AML preclinical models. Moreover, it synergizes with AZA, a DNA hypomethylating agent widely used for AML treatment. TAK-981 and AZA combo induces a broad transcriptional reprogramming of AML cells underlying pleiotropic effects. These include increased apoptosis, alteration of the cell cycle, differentiation of the leukemic cells, induction of IFN-I secretion and enhanced expression of NK cell ligands at the surface of AML cells, which stimulates NK cytotoxicity towards them (Figure 8).

Accumulating evidence suggest that alteration in SUMOylation can both contribute to tumorigenesis and affect response to therapies in various cancers.[36] This is notably the case for AML.[37] Different inhibitors of SUMOylation such as anacardic acid,[17] 2D-08[18,38] and McM025044[39] showed *in vitro* toxicity for leukemic cell. However, their low activity (μM range) and poor pharmacological properties prevented further preclinical studies. The discovery of TAK-981 now

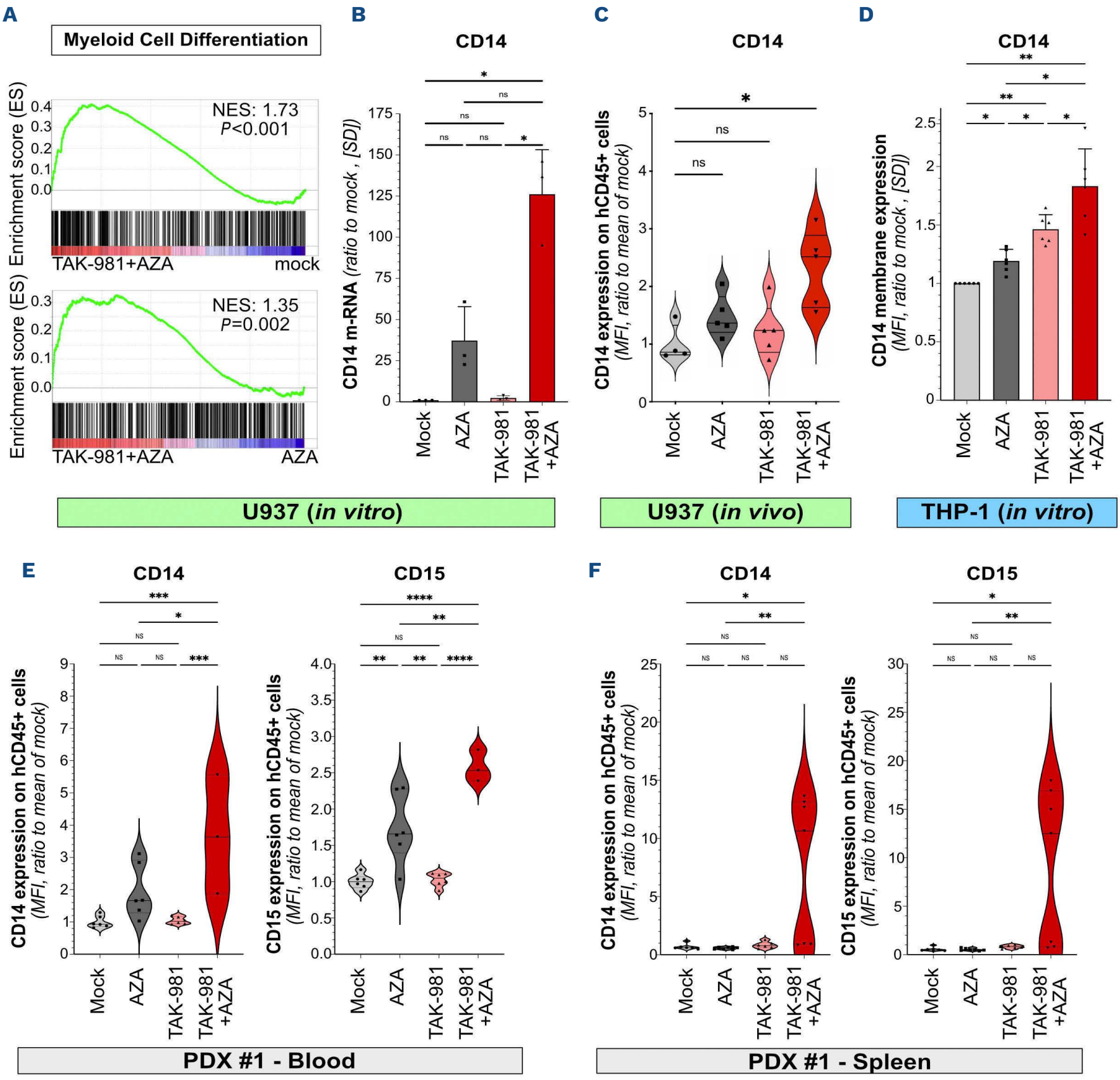

Figure 5. TAK-981+5-azacytidine induces differentiation of acute myeloid leukemia cells. (A) Gene set enrichment analysis enrichment plot for the gene signature "GOBP Myeloid Cell Differentiation" in TAK-981+5-azacytidine [AZA]-treated U937 cells compared to mock- (upper panel) or AZA- (lower panel) treated cells. (B) mRNA expression of *CD14* was analyzed by quantitative reverse transcription polymerase chain reaction (qRT-PCR) in U937 cells treated for 72 hours with 10 nM AZA, 10 nM TAK-981 or the drug combination. Results were normalized to *GAPDH* mRNA levels and expressed as ratio to mock-treated cells (N=3, mean +/- standard deviation [SD], conditions were compared using RM one-way ANOVA test). (C) NSG mice were injected with U937 cells (N=4 or 5/group) and, after engraftment, treated according to treatment schedule presented in Figure 2A. Bone marrow were collected at day 9 after treatment start and the level of CD14 was assessed by flow cytometry at cell surface of hCD45$^+$ cells. Data were normalized to the mean of CD14 expression (mean fluorescence intensity [MFI]) in mock-treated group of mice. For each group, plain lines represent the median value and dotted lines are the quartiles. Groups were compared using Ordinary one-way ANOVA test. (D) Expression of CD14 was measured by flow cytometry on THP-1 treated with 10 nM AZA, 10 nM TAK-981 or the drug combination for 72 hours. MFI were normalized to that of mock-treated cells (N=6, mean +/- SD, RM one-way ANOVA test). (E, F) NSG mice were injected with primary patient cells (PDX #1), and treated according to treatment schedule presented in Figure 2A. Peripheral blood samples (N=3-6/group) were collected at day 30 after treatment start (E) or, in an independent experiment, spleens (N=6 or 7/group) were collected at day 9 after treatment start (F). The level of CD14 and CD15 protein expression at cell surface of hCD45$^+$ cells was evaluated by flow cytometry. Data were normalized on the mean of CD14 and CD15 expression (MFI) in cells from the mock-treated group. For each group, plain lines represent the median values, and dotted lines are the quartiles. Groups were compared using Kruskall-Wallis test, due to lack of normality of data.

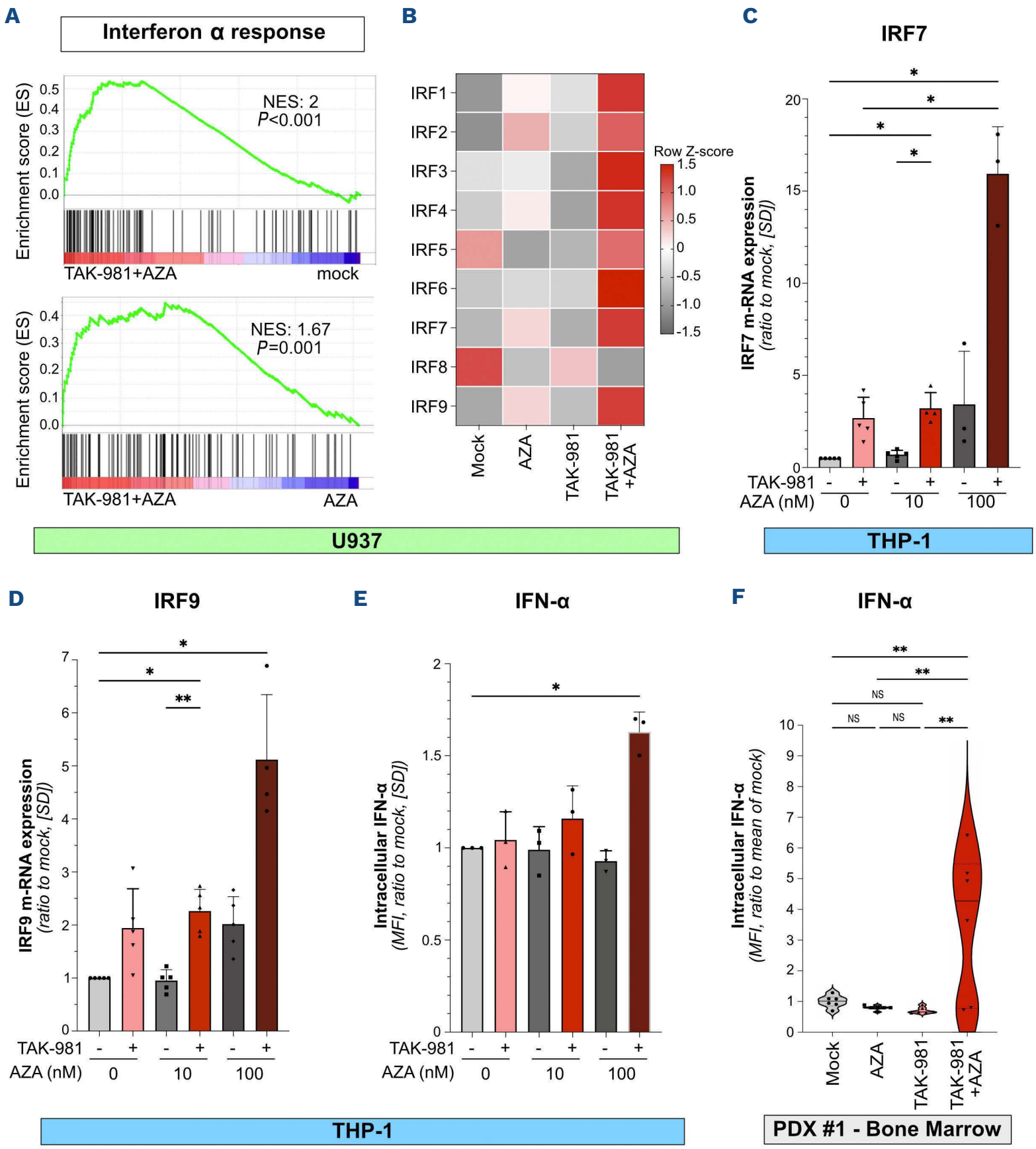

Figure 6. TAK-981 and 5-azacytidine combination activates type-1 interferon secretion by acute myeloid leukemia cells. (A) Gene set enrichment analysis plot for genes involved in interferon α (IFN-α) response in TAK-981+AZA treated U937 cells compared to mock- (upper panel) and 5-azacytidine (AZA)- (lower panel) treated cells. (B) Heatmap representing the RNA-sequencing results for the expression of interferon regulatory factor (IRF) in U937 cells. (C, D) mRNA expression of *IRF7* (C) and *IRF9* (D) was analyzed by quantitative reverse transcription polymerase chain reaction (qRT-PCR) in THP-1 cells treated for 72 hours with 10 nM TAK-981 and the indicated concentrations of AZA. Results were normalized to *GAPDH* mRNA levels and expressed as ratio to mock-treated cells (N=3-5, mean +/- standard deviation [SD], all conditions were compared using RM one-way ANOVA test, only those with significant *P* values are shown). (E) THP-1 cells were treated for 3 consecutive days with TAK-981 (10 nM) and/or AZA (10 nM or 100 nM). After 8 days, cells were collected and the production of intracellular IFN-α was analyzed by flow cytometry. Background was subtracted and data normalized to the mock-treated condition (N=3, mean +/- SD, all conditions were compared using RM one-way ANOVA test, only those with significant *P* values are shown). (F) NSG mice were injected with primary patient cells (PDX #1) and treated according to treatment schedule presented in Figure 2A. Spleens (N=6/group) were collected at day 9 after treatment start and the level of intracellular IFN-α in hCD45$^+$ cells was assessed by flow cytometry. Data were normalized to the mean of IFN-α expression (mean fluorescence intensity [MFI]) in mock-treated group of mice. For each group, plain lines represent the median value and dotted lines are the quartiles. Groups were compared using ordinary one-way ANOVA test.

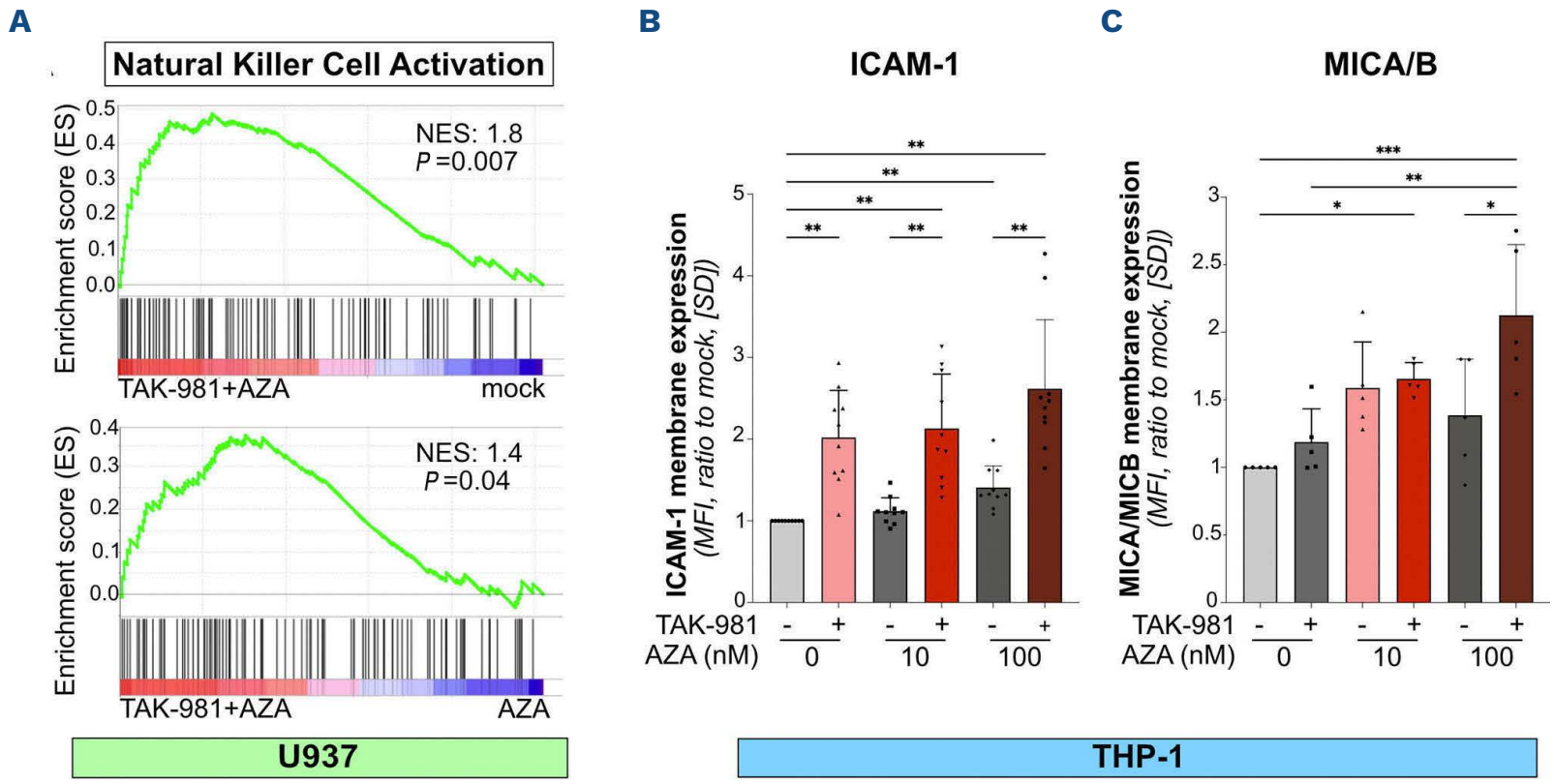

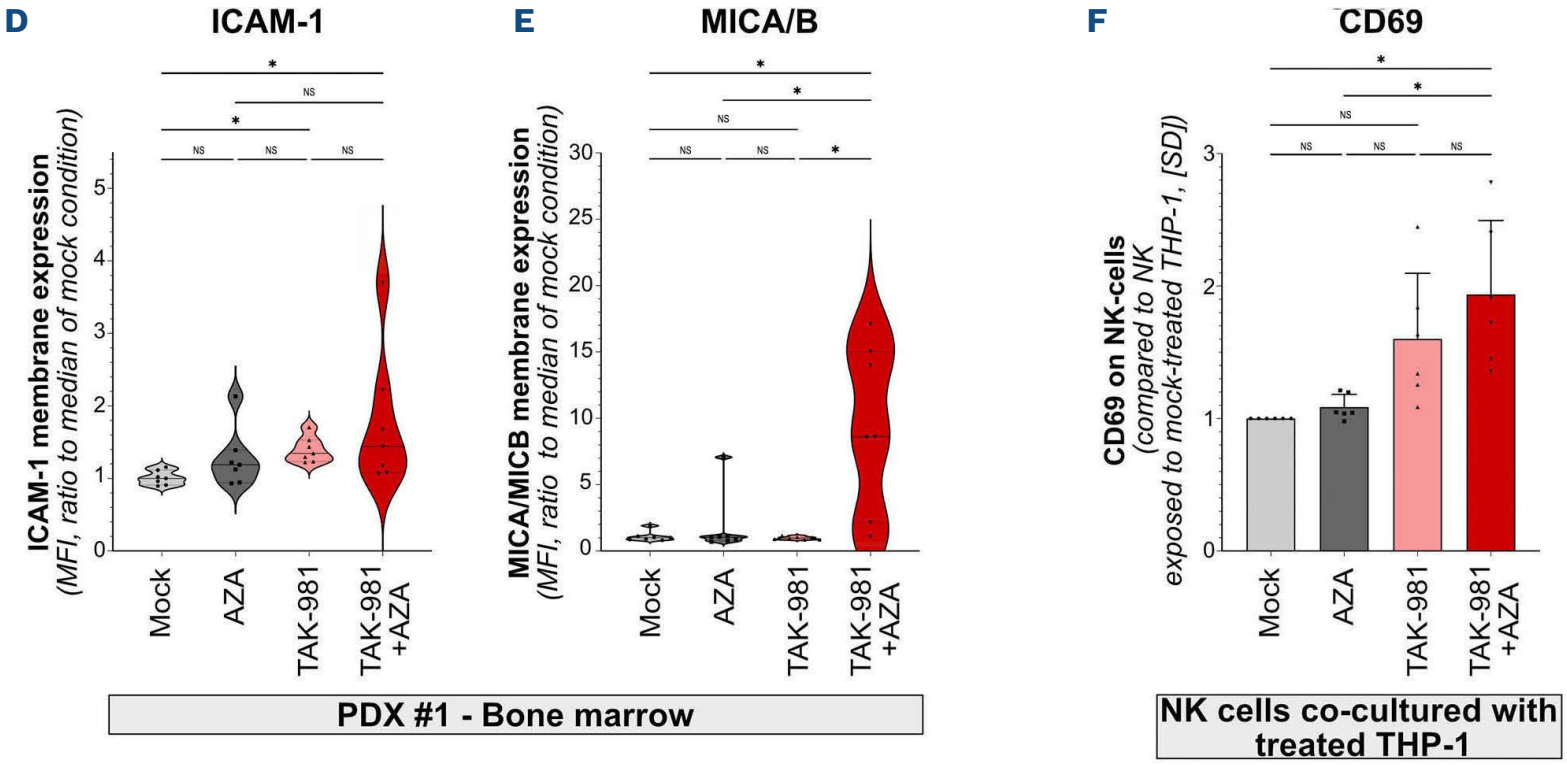

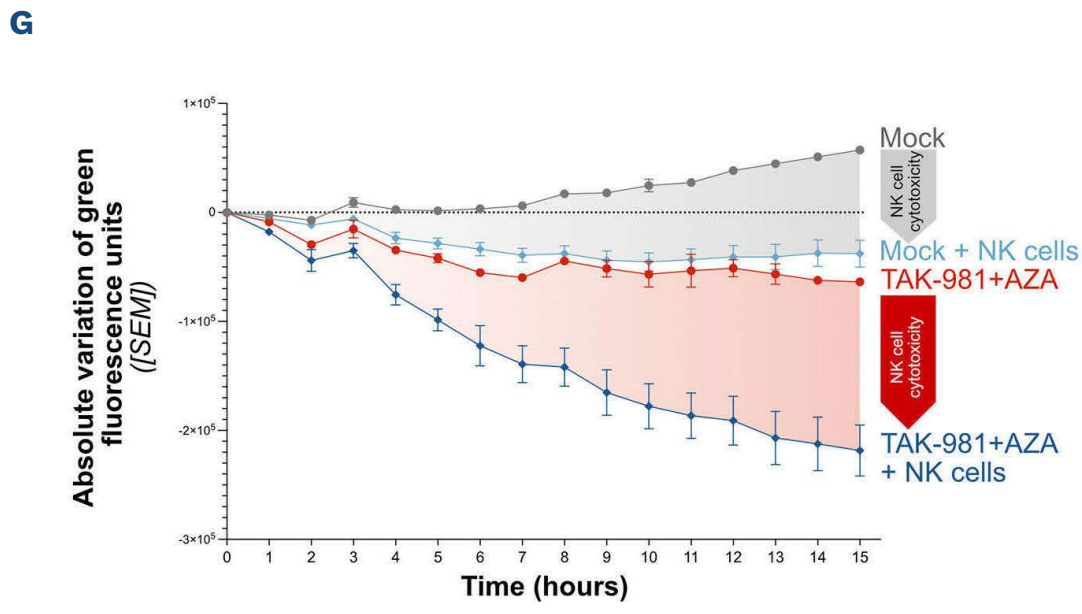

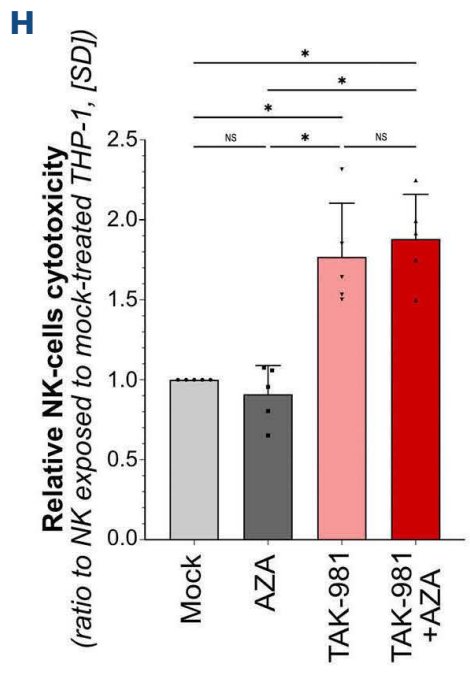

Continued on following page.

Figure 7. TAK-981 treatment of acute myeloid leukemia cells leads to natural killer cell activation and increased natural killer cell cytotoxicity. (A) Gene set enrichment analysis enrichment plot for genes involved in natural killer (NK) cell-mediated cytotoxicity in TAK-981+5-azacytidine (AZA)-treated U937 cells compared to mock- (upper panel) or AZA- (lower panel) treated cells. (B, C) Expression of ICAM-1 (B) and MICA/B (C) was measured by flow cytometry on THP-1 treated with 10 nM TAK-981 and AZA at the indicated concentrations for 72 hours. Background was subtracted and results were normalized to mock-treated condition (N=10 for ICAM-1, N=5 for MICA/B, mean +/- standard deviation [SD], RM one-way ANOVA test). (D, E) NSG mice (N=7/group) were injected with primary patient cells (PDX #1), and treated according to treatment schedule presented in Figure 2A. Bone marrows were collected at day 9 after treatment start and ICAM-1 and MICA/B expression on the membrane of human $CD45^+$ cells was assessed by flow cytometry. Data were normalized to the mean fluorescence intensity (MFI) of mock-treated mice group. Plain lines represent the median values, and dotted lines are the quartiles. Groups were compared using Kruskall-Wallis test. (F) THP-1 cells were treated each day for 3 consecutive days with 10 nM AZA, 10 nM TAK-981 or the drug combination, and co-cultured at day 8 with healthy donor peripheral blood mononuclear cells (PBMC) at a 1:10 acute myeloid leukemia (AML):PBMC ratio. After 24 hours of co-culture, expression of activation marker CD69 was assessed by flow cytometry on NK cells ($CD3^-/CD56^+$ cells). Data were normalized to the MFI of CD69 expression on NK cells co-cultured with untreated THP-1, (mean +/- SD, N=6, RM one-way ANOVA test). (G, H) Real-time immune cell killing assay. To evaluate NK cells cytotoxicity against AML cells treated with TAK-981-/+AZA, co-culture experiments were performed during 15 hours using an Incucyte device between, on one hand, THP-1-Luc-ZsGreen cells previously treated for 72 hours with 10 nM AZA, 10 nM TAK-981 or the drug combination, and on the other hand, NK cells, purified from healthy donor PBMC. Cells were used at a 1:1 AML:NK ratio. (G) Relative green fluorescence intensities for THP-1-Luc-ZsGreen cells mock-treated without (grey curve) or with NK cells (light blue curve) and treated with TAK-981+AZA without (red curve) or with NK cells (dark blue curve) (N=5). Cytotoxicity of NK cells was calculated by comparing grey- (mock-treated THP-1-/+NK cells) and red areas (AZA+TAK-981 treated THP-1-/+NK cells). (H) NK cells cytotoxicity was determined by calculating areas between the curves for each treatment condition (10 nM AZA, 10 nM TAK-981 or the drug combination) with or without NK. Data were normalized to mock-treated THP-1 cells (N=5, mean +/- SD, RM one-way ANOVA test).

allows to envision SUMOylation inhibition in cancer patients. Five phase I/II clinical trials are ongoing in solid tumors (*clinicaltrials gov. Identifier: NCT03648372, NCT04381650*), multiple myelomas (*clinicaltrials gov. Identifier: NCT04776018*) and lymphomas (*clinicaltrials gov. Identifier: NCT03648372, NCT04074330*). Our data obtained in preclinical models of AML provide a rationale for evaluating TAK-981 in AML treatment. Importantly, we observed minimal toxicity of TAK-981 on normal blood and BMMC (Figure 1C, G) or when administered to mice (Figure 2).

Although TAK-981 can kill leukemic cells *in vitro* and *in vivo*, its anti-tumor activity is relatively limited when used as monotherapy. However, its combination with AZA has a largely superior anti-leukemic activity. Combination therapies are increasingly considered to achieve stronger responses to cancer treatments and to limit relapses, including in AML.[40] This notably concerns AZA, whose combination with various drugs, in particular VEN, has improved clinical responses.[3] Nevertheless, many patients are refractory to VEN+AZA regimen or relapse after treatment.[9,10] This is for example the case of patients suffering from monocytic AML (FAB M4 and M5).[41] It is, therefore, interesting that TAK-981+AZA shows more efficiency than VEN+AZA for all cell lines tested. In particular, TAK-981+AZA was more efficient than VEN+AZA at inducing apoptosis, cell cycle defects and differentiation of the monocytic cell lines U937 and THP-1. In addition, in our *in vitro* experiments on patient cells (Figure 1F; *Online Supplementary Figure S2B*), AML cells from the more differentiated M4 and M5 subgroups were as sensitive (even slightly more sensitive) to TAK-981+AZA treatment than less differentiated AML cells from the M1 and M2 subgroups. Patients who are refractory to VEN+AZA regimen might therefore be sensitive to TAK-981+AZA treatment.

The synergy between AZA and TAK-981 likely resides in the ability of TAK-981 to enhance the action of AZA on transcription. A large number of transcription factors, co-activators and co-repressor complexes, the basal transcription machinery and histones are SUMOylated.[15,16,42] In general, SUMOylation of protein complexes rather than individual proteins within these complexes mediates the biological effects of SUMOylation, which include the stabilization of these complexes[43] or the recruitment of SUMO interacting motif (SIM)-containing proteins.[44,45] For example, SUMOylation of chromatin bound proteins can favor the recruitment of co-repressor complexes such as those containing histone deacetylases (HDAC)[46-48] or the histone methyl transferase SETDB1[49] via SUMO-SIM interactions. We show that inhibition of SUMOylation *per se* has limited effects on gene expression. Although surprising considering the high number of SUMOylated proteins present on gene regulatory regions, SUMOylation is thus dispensable for gene expression in basal conditions. However, inhibition of SUMOylation largely increases the expression of most AZA-induced genes. Hence, it is likely that the effect of TAK-981 on AZA-induced transcriptional reprogramming is due to the global deSUMOylation of proteins bound to gene regulatory regions rather than the consequence of the deSUMOylation of specific proteins present in these regions. This deSUMOylation would create a permissive environment for transcription, likely by affecting the recruitment and activity of transcription regulating- and/or chromatin remodeling-complexes. This would, therefore, amplify the transcriptional regulation of genes, whose *cis*-regulatory regions have been hypo-methylated by AZA. Of note, we have recently shown that inhibition of SUMOylation limits the transcriptional reprogramming induced by DNR in AML cells after few hours of treatment.[50] This suggests that inhibitors of SUMOylation could have different global impacts on gene expression depending on the duration of

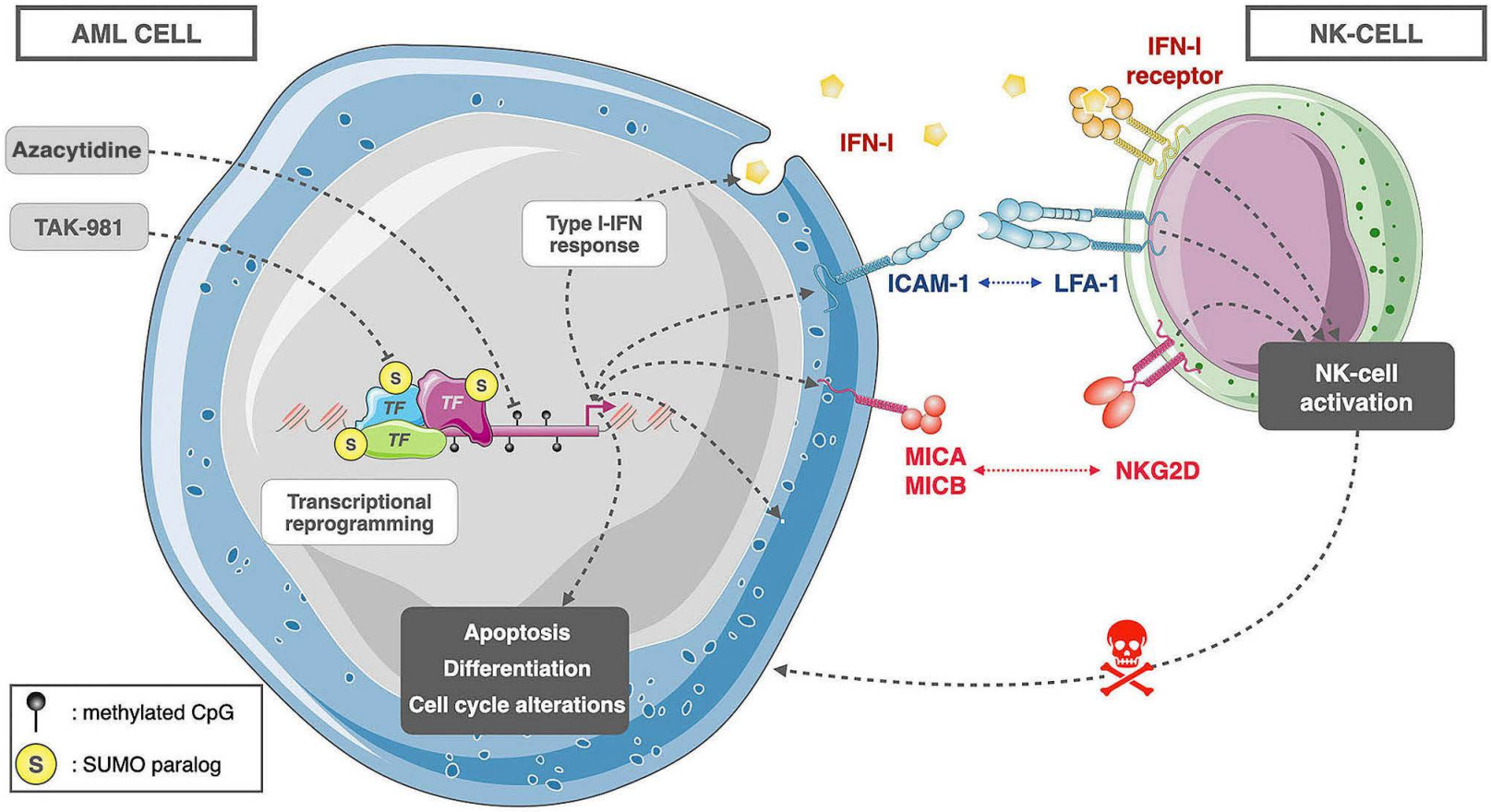

Figure 8. Model for the anti-leukemic activity of TAK-981+5-azacytidine in acute myeloid leukemia. Combined inhibition of SUMOylation with TAK-981 and DNA methylation with 5-azacytidine (AZA) induces a transcriptional reprogramming in acute myeloid leukemia (AML) cells. This includes the activation of genes involved in the induction of apoptosis and differentiation and a repression of genes linked to cell cycle progression. In addition, TAK-981+AZA induces interferon 1 (IFN-1) secretion as well as the expression of natural killer (NK) cell ligands at the surface of acute myeloid leukemia (AML) cells. This activates NK and increases their cytotoxicity towards AML cells.

the treatment (hours *vs*. days) and/or the drugs they are associated with.

We also do not exclude that other mechanisms than transcriptional reprogramming might be at play to explain the synergy between AZA and TAK-981. Poly-SUMOylation of DNMT1 was shown to be triggered by decitabine, another hypomethylating agent, which induces crosslink between DNMT1 and DNA. This leads to its RNF4-mediated ubiquitylation and promotes the resolution of the DNA-protein crosslinks (DPC).[4,51] Accordingly, inhibition of SUMOylation increases decitabine-induced DPC, ultimately resulting in DNA damage and cell death in models of lymphoma.[52] However, these studies were performed with high doses (1-10 μM) of decitabine, which is much more prone to induce DPC and DNA damage than AZA at the same doses.[53] In the condition used in our transcriptomic study (10 nM of AZA for 72 hours), it is unlikely that AZA induces massive DPC and subsequent DNA damage. Moreover, the transcriptional reprogramming we characterized in AML was observed at sublethal doses of the drugs, further supporting the idea that it did not involve DPC-induced DNA damages.

Our data point to pleiotropic effects of the TAK-981+AZA combo to eliminate AML cells through increased apoptosis, decreased proliferation and induction of myeloid differentiation. The contribution of these different pathways to the anti-leukemic activity of the TAK-981+AZA combo differs depending on the concentrations of the drugs. At the highest doses, apoptosis is likely central to the anti-leukemic action of TAK-981+AZA. At lower doses, differentiation might be the main contributor to the decreased cell proliferation upon TAK-981+AZA treatment. Indeed, induction of differentiation is critical for the action of various AML therapies, including all *trans* retinoic acid (ATRA) and arsenic trioxide in acute promyelocytic leukemia (APL) subtype of AML[54] as well as IDH1 and FLT3 inhibitors.[55]

In addition to the direct effect on AML cells proliferation and survival, TAK-981+AZA combination induces many genes linked to inflammation and immunity. This is notably the case for the IFN-I pathway, which has been reported to be activated by both AZA in cancer cells[56,57] and by TAK-981 in immune cells.[20,21] IFN-I induction can then induce an anti-tumor immune response in these models.[20,21,23] Although TAK-981 on its own weakly induced IFN-I pathway, its combination with AZA largely increased IFN-I secretion by AML cells themselves. Although systemic IFN-I based therapies have proven disappointing in terms of clinical efficacy with important toxicities,[58] controlled and localized secretion of IFN-I by AML cells might be sufficient to elicit an anti-leukemic immune response devoid of toxicity.

Finally, our work suggests an important role for NK cells in the elimination of TAK-981-treated AML cells. NK cells can eliminate tumor cells directly by inducing their lysis or indirectly through the secretion of cytokines such as

IFN-γ or TNF-α. AML patients survival is highly correlated with the number and activity of NK cells.[35] However, NK cells are often poorly functional in these patients. In particular, NK cells from AML patients are often defective in the expression of activating receptors (DNAM1, NKp30, NKp46) or overexpress inhibitory KIR receptors. Finally, AML cells develop immunosuppressive strategies to escape NK cell-mediated cell lysis, such as downregulation or shedding from their cell surface of ligands of the NK cell-activating receptor NKG2D (MICA/MICB and ULBP1-6).[35] It was, therefore, interesting to observe that TAK-981+AZA treatment leads to upregulation of MICA/MICB at the surface of AML cells. In addition, we also detected an upregulation of adhesion molecule ICAM-1, whose binding to the LFA-1 receptor on NK cells is required for efficient lysis of AML cells.[34] The combined secretion of cytokines and expression of NK cell-activating markers by AML cells could explain the increased activation and enhanced cytotoxicity of NK cells towards TAK-981+AZA-treated AML cells.

In conclusion, our work suggests that targeting SUMOylation with TAK-981 may be a promising strategy to enhance the clinical efficacy of AZA in AML patients. This combination treatment is expected to exert cell-autonomous effects on AML cells by inducing their differentiation and apoptosis and cell-extrinsic effects by triggering an anti-leukemic immune response.

Disclosures

TAK-981 was obtained from Takeda Development Center Americas, Inc. GC is a consultant for Roche and BMS-Celgene; is a member of the advisory boards of MabQi, Ownards Therapeutics, MedXcell and receives honoraria from Abbvie, Sanofi, Gilead, Janssen, Roche, BMS-Celgene, Takeda Pharmaceuticals. The remaining authors have no conflicts of interest to disclose.

Contributions

LG designed and performed the experiments on cell lines, patient cells and mouse models. MDT conceived and performed in vivo experiments. MC prepared samples for RNA-sequencing and performed qPCR. DA, MA and GiB analyzed viability and differentiation of AML cell lines. RH participated in PBMC and NK purifications. MA, RH and DA performed validation qPCR. AD prepared RNA-sequencing libraries and sequenced them. CRZ performed microbead-based assay. GC provided patient samples. DT conceived and analyzed RNA-sequencing experiments and performed GSEA analysis. MP provided funding for the study. GB supervised the study and provided funding. LG, MDT, DT, MP and GB wrote the manuscript.

Acknowledgments

We thank the members of the "Ubiquitin Family in Hematological Malignancies" group, Takeda Development Center Americas (Lexington, MA), for providing TAK-981 and Dr Allison Berger for critically reading the manuscript.

Funding

Funding was provided by the CNRS, the Ligue Nationale contre le Cancer (to DA, MC, MP), the Fondation pour la Recherche Médicale (contract FDM201906008566, LG), INCa_16072, the Fédération Leucémie Espoir, the Association Laurette Fugain, the Fondation ARC pour la recherche sur le cancer and the Agence Nationale pour la Recherche ("Investissements d'avenir" program; ANR-16-IDEX-0006; project SUMOLAM). The HEMODIAG_2020 collection was funded by the Montpellier University Hospital, the Montpellier SIRIC and the Languedoc Roussillon Region. MGX acknowledges financial support from the France Génomique National infrastructure, funded as part of "Investissements d'Avenir" program managed by the Agence Nationale pour la Recherche (contract ANR 10 INBS 09).

Data-sharing statement

The RNA-sequencing data are available on Gene Expression Omnibus with accession number GSE212330. All other data are presented in the main text or the Online Supplementary Appendix.

References

1. Saultz JN, Garzon R. Acute myeloid leukemia: a concise review. J Clin Med. 2016;5(3):33.
2. Ahmadmehrabi K, Haque AR, Aleem A, Griffiths EA, Roloff GW. Targeted therapies for the evolving molecular landscape of acute myeloid leukemia. Cancers (Basel). 2021;13(18):4646.
3. Ciotti G, Marconi G, Martinelli G. Hypomethylating agent-based Ccmbination therapies to treat post-hematopoietic stem cell transplant relapse of acute myeloid leukemia. Front Oncol. 2022;11:810387.
4. Liu JCY, Kühbacher U, Larsen NB, et al. Mechanism and function of DNA replication-independent DNA-protein crosslink repair via the SUMO-RNF4 pathway. EMBO J. 2021;40(18):e107413.
5. Lund K, Cole JJ, VanderKraats ND, et al. DNMT inhibitors reverse a specific signature of aberrant promoter DNA methylation and associated gene silencing in AML. Genome Biol. 2014;15(8):406.
6. Dombret H, Seymour JF, Butrym A, et al. International phase 3 study of azacitidine vs conventional care regimens in older patients with newly diagnosed AML with >30% blasts. Blood. 2015;126(3):291-299.
7. DiNardo CD, Pratz K, Pullarkat V, et al. Venetoclax combined with decitabine or azacitidine in treatment-naive, elderly patients with acute myeloid leukemia. Blood. 2019;133(1):7-17.
8. DiNardo CD, Jonas BA, Pullarkat V, et al. Azacitidine and venetoclax in previously untreated acute myeloid leukemia. N Engl J Med. 2020;383(7):617-629.

9. Garciaz S, Saillard C, Hicheri Y, Hospital M-A, Vey N. Venetoclax in acute myeloid leukemia: molecular basis, evidences for preclinical and clinical efficacy and strategies to target resistance. Cancers. 2021;13(22):5608.
10. Ong F, Kim K, Konopleva MY. Venetoclax resistance: mechanistic insights and future strategies. Cancer Drug Resist. 2022;5(2):380-400.
11. Vertegaal ACO. Signalling mechanisms and cellular functions of SUMO. Nat Rev Mol Cell Biol. 2022;23(11):715-731.
12. Hendriks IA, Lyon D, Young C, Jensen LJ, Vertegaal ACO, Nielsen ML. Site-specific mapping of the human SUMO proteome reveals co-modification with phosphorylation. Nat Struct Mol Biol. 2017;24(3):325-336.
13. Hendriks IA, Lyon D, Su D, et al. Site-specific characterization of endogenous SUMOylation across species and organs. Nat Commun. 2018;9(1):2456.
14. Pichler A, Fatouros C, Lee H, Eisenhardt N. SUMO conjugation - a mechanistic view. Biomol Concepts. 2017;8(1):13-36.
15. Boulanger M, Chakraborty M, Tempé D, Piechaczyk M, Bossis G. SUMO and transcriptional regulation: the lessons of large-scale proteomic, modifomic and genomic studies. Molecules. 2021;26(4):828.
16. Rosonina E. A conserved role for transcription factor sumoylation in binding-site selection. Curr Genet. 2019;65(6):1307-1312.
17. Bossis G, Sarry J-E, Kifagi C, et al. The ROS/SUMO axis contributes to the response of acute myeloid leukemia cells to chemotherapeutic drugs. Cell Rep. 2014;7(6):1815-1823.
18. Baik H, Boulanger M, Hosseini M, et al. Targeting the SUMO pathway primes all-trans retinoic acid–induced differentiation of nonpromyelocytic acute myeloid leukemias. Cancer Res. 2018;78(10):2601-2613.
19. Langston SP, Grossman S, England D, et al. Discovery of TAK-981, a first-in-class inhibitor of SUMO-activating enzyme for the treatment of cancer. J Med Chem. 2021;64(5):2501-2520.
20. Lightcap ES, Yu P, Grossman S, et al. A small-molecule SUMOylation inhibitor activates antitumor immune responses and potentiates immune therapies in preclinical models. Sci Transl Med. 2021;13(611):eaba7791.
21. Kumar S, Schoonderwoerd MJA, Kroonen JS, et al. Targeting pancreatic cancer by TAK-981: a SUMOylation inhibitor that activates the immune system and blocks cancer cell cycle progression in a preclinical model. Gut. 2022;71(11):2266-2283.
22. Demel UM, Böger M, Yousefian S, et al. Activated SUMOylation restricts MHC class I antigen presentation to confer immune evasion in cancer. J Clin Invest. 2022;132(9):e152383.
23. Nakamura A, Grossman S, Song K, et al. SUMOylation inhibitor subasumstat potentiates rituximab activity by IFN1-dependent macrophage and NK cell stimulation. Blood. 2022;139(18):2770-2781.
24. Demel UM, Wirth M, Yousefian S, et al. Small molecule SUMO inhibition for biomarker-informed B-cell lymphoma therapy. Haematologica. 2023;108(2):555-567.
25. Du L, Liu W, Pichiorri F, Rosen ST. SUMOylation inhibition enhances multiple myeloma sensitivity to lenalidomide. Cancer Gene Ther. 2022;30(4):567-574.
26. Du L, Liu W, Aldana-Masangkay G, et al. SUMOylation inhibition enhances dexamethasone sensitivity in multiple myeloma. J Exp Clin Cancer Res. 2022;41(1):1-16.
27. Kim HS, Kim B-R, Dao TTP, et al. TAK-981, a SUMOylation inhibitor, suppresses AML growth immune-independently. Blood Adv. 2023;7(13):3155-3168.
28. Paolillo R, Boulanger M, Gâtel P, et al. The NADPH oxidase NOX2 is a marker of adverse prognosis involved in chemoresistance of acute myeloid leukemias. Haematologica. 2022;107(11):2562-2575.
29. Gâtel P, Brockly F, Reynes C, et al. Ubiquitin and SUMO conjugation as biomarkers of acute myeloid leukemias response to chemotherapies. Life Sci Alliance. 2020;3(6):e201900577.
30. Recasens-Zorzo C, Gâtel P, Brockly F, Bossis G. A microbead-based flow cytometry assay to assess the activity of ubiquitin and ubiquitin-like conjugating enzymes. Methods Mol Biol. 2023;2602:65-79.
31. Gartel AL, Ye X, Goufman E, et al. Myc represses the p21(WAF1/CIP1) promoter and interacts with Sp1/Sp3. Proc Natl Acad Sci U S A. 2001;98(8):4510-4515.
32. Stubbins RJ, Karsan A. Differentiation therapy for myeloid malignancies: beyond cytotoxicity. Blood Cancer J. 2021;11(12):1-9.
33. Rahmani S, Yazdanpanah N, Rezaei N. Natural killer cells and acute myeloid leukemia: promises and challenges. Cancer Immunol Immunother. 2022;71(12):2849-2867.
34. Allende-Vega N, Marco Brualla J, Falvo P, et al. Metformin sensitizes leukemic cells to cytotoxic lymphocytes by increasing expression of intercellular adhesion molecule-1 (ICAM-1). Sci Rep. 2022;12(1):1341.
35. Carlsten M, Järås M. Natural killer cells in myeloid malignancies: immune surveillance, NK cell dysfunction, and pharmacological opportunities to bolster the endogenous NK cells. Front Immunol. 2019;10:2357.
36. Seeler J-S, Dejean A. SUMO and the robustness of cancer. Nat Rev Cancer. 2017;17(3):184-197.
37. Boulanger M, Paolillo R, Piechaczyk M, Bossis G. The SUMO pathway in hematomalignancies and their response to therapies. Int J Mol Sci. 2019;20(16):3895.
38. Zhou P, Chen X, Li M, et al. 2-D08 as a SUMOylation inhibitor induced ROS accumulation mediates apoptosis of acute myeloid leukemia cells possibly through the deSUMOylation of NOX2. Biochem Biophys Res Commun. 2019;513(4):1063-1069.
39. Benoit YD, Mitchell RR, Wang W, et al. Targeting SUMOylation dependency in human cancer stem cells through a unique SAE2 motif revealed by chemical genomics. Cell Chem Biol. 2021;28(10):1394-1406.
40. Ishii H, Yano S. New therapeutic strategies for adult acute myeloid leukemia. Cancers (Basel). 2022;14(11):2806.
41. Pei S, Pollyea DA, Gustafson A, et al. Monocytic subclones confer resistance to venetoclax-based therapy in patients with acute myeloid leukemia. Cancer Discov. 2020;10(4):536-551.
42. Ryu H-Y, Hochstrasser M. Histone sumoylation and chromatin dynamics. Nucleic Acids Res. 2021;49(11):6043-6052.
43. Seifert A, Schofield P, Barton GJ, Hay RT. Proteotoxic stress reprograms the chromatin landscape of SUMO modification. Sci Signal. 2015;8(384):rs7.
44. González-Prieto R, Eifler-Olivi K, Claessens LA, et al. Global non-covalent SUMO interaction networks reveal SUMO-dependent stabilization of the non-homologous end joining complex. Cell Rep. 2021;34(4):108691.
45. Lascorz J, Codina-Fabra J, Reverter D, Torres-Rosell J. SUMO-SIM interactions: from structure to biological functions. Semin Cell Dev Biol. 2022;132:193-202.
46. Ouyang J, Shi Y, Valin A, Xuan Y, Gill G. Direct binding of CoREST1 to SUMO-2/3 contributes to gene-specific repression by the LSD1/CoREST1/HDAC complex. Mol Cell. 2009;34(2):145-154.
47. Hua G, Ganti KP, Chambon P. Glucocorticoid-induced tethered transrepression requires SUMOylation of GR and formation of a

SUMO-SMRT/NCoR1-HDAC3 repressing complex. Proc Natl Acad Sci U S A. 2016;113(5):E635-E643.
48. Pascual G, Fong AL, Ogawa S, et al. A SUMOylation-dependent pathway mediates transrepression of inflammatory response genes by PPAR-γ. Nature. 2005;437(7059):759-763.
49. Ivanov AV, Peng H, Yurchenko V, et al. PHD domain-mediated E3 ligase activity directs intramolecular sumoylation of an adjacent bromodomain required for gene silencing. Mol Cell. 2007;28(5):823-837.
50. Boulanger M, Aqrouq M, Tempé D, et al. DeSUMOylation of chromatin-bound proteins limits the rapid transcriptional reprogramming induced by daunorubicin in acute myeloid leukemias. Nucleic Acids Res. 2023;51(16):8413-8433.
51. Borgermann N, Ackermann L, Schwertman P, et al. SUMOylation promotes protective responses to DNA-protein crosslinks. EMBO J. 2019;38(8):e101496.
52. Kroonen JS, de Graaf IJ, Kumar S, et al. Inhibition of SUMOylation enhances DNA hypomethylating drug efficacy to reduce outgrowth of hematopoietic malignancies. Leukemia. 2023;37(4):864-876.
53. Hollenbach PW, Nguyen AN, Brady H, et al. A comparison of azacitidine and decitabine activities in acute myeloid leukemia cell lines. PLoS One. 2010;5(2):e9001.
54. Yilmaz M, Kantarjian H, Ravandi F. Acute promyelocytic leukemia current treatment algorithms. Blood Cancer J. 2021;11(6):1-9.
55. Madan V, Koeffler HP. Differentiation therapy of myeloid leukemia: four decades of development. Haematologica. 2021;106(1):26-38.
56. Roulois D, Loo Yau H, Singhania R, et al. DNA-demethylating agents target colorectal cancer cells by inducing viral mimicry by endogenous transcripts. Cell. 2015;162(5):961-973.
57. Chiappinelli KB, Strissel PL, Desrichard A, et al. Inhibiting DNA Methylation causes an interferon response in cancer via dsRNA including endogenous retroviruses. Cell. 2015;162(5):974-986.
58. Aricò E, Castiello L, Capone I, Gabriele L, Belardelli F. Type I interferons and cancer: an evolving story demanding novel clinical applications. Cancers (Basel). 2019;11(12):1943.